# Influence of optical forces on nonlinear optical frequency conversion in nanoscale waveguide devices

**Zhen-xing Wu, Wei Luo, Shi-han Tang, Fei Xu,* and Yan-qing Lu**

*National Laboratory of Solid State Microstructures and College of Engineering and Applied Science, Nanjing University, Nanjing 210093, China*
**feixu@nju.edu.cn*

**Abstract:** We theoretically investigate the influence of optical gradient forces on nonlinear frequency conversion in a typical nanoscale optomechanical system, which consists of two parallel, suspended waveguides. The waveguides deform with the input power and the phase-matching wavelength changes along the waveguides. Utilizing the spread of deformations collectively allows phase matching over a wider range of pump wavelengths. The third harmonic phase-matching wavelength shift can be as large as 3.6 nm/mW when the waveguide length is 100 μm and the initial gap is 150 nm. It is analogous to chirping the poling period of quasi-phase-matched devices to extend their bandwidths, and allows broad third harmonic to be generated for uses such as biological spectroscopy. Finally, we discuss the conversion efficiency and the optimal phase-matching wavelength with a single-frequency pump.



**OCIS codes:** (120.4880) Optomechanics; (130.3120) Integrated optics devices; (190.2620) Harmonic generation and mixing.

## References and links

1. T. Corbitt, D. Ottaway, E. Innerhofer, J. Pelc, and N. Mavalvala, "Measurement of radiation-pressure-induced optomechanical dynamics in a suspended Fabry-Perot cavity," Phys. Rev. A **74**(2), 021802 (2006).
2. F. Riboli, A. Recati, M. Antezza, and I. Carusotto, "Radiation induced force between two planar waveguides," Eur. Phys. J. D **46**(1), 157–164 (2008).
3. G. S. Wiederhecker, L. Chen, A. Gondarenko, and M. Lipson, "Controlling photonic structures using optical forces," Nature **462**(7273), 633–636 (2009).
4. J. Ma and M. L. Povinelli, "Mechanical Kerr nonlinearities due to bipolar optical forces between deformable silicon waveguides," Opt. Express **19**(11), 10102–10110 (2011).
5. B. Zheng, W. Luo, F. Xu, and Y. Lu, "Influence of van der Waals forces on the waveguide deformation and power limit of nanoscale waveguide devices," Phys. Rev. A **89**(4), 043810 (2014).
6. J. Ma and M. L. Povinelli, "Large tuning of birefringence in two strip silicon waveguides via optomechanical motion," Opt. Express **17**(20), 17818–17828 (2009).
7. K. Y. Fong, W. H. Pernice, M. Li, and H. X. Tang, "Tunable optical coupler controlled by optical gradient forces," Opt. Express **19**(16), 15098–15108 (2011).
8. Y. Vlasov, W. M. J. Green, and F. Xia, "High-throughput silicon nanophotonic wavelength-insensitive switch for on-chip optical networks," Nat. Photonics **2**(4), 242–246 (2008).
9. J. L. Kou, Q. Wang, Z. Y. Yu, F. Xu, and Y. Q. Lu, "Broadband and highly efficient quadratic interactions in double-slot lithium niobate waveguides through phase matching," Opt. Lett. **36**(13), 2533–2535 (2011).
10. T. Lee, Y. Jung, C. A. Codemard, M. Ding, N. G. Broderick, and G. Brambilla, "Broadband third harmonic generation in tapered silica fibres," Opt. Express **20**(8), 8503–8511 (2012).
11. R. P. Schmid, T. Schneider, and J. Reif, "Optical processing on a femtosecond time scale," Opt. Commun. **207**(1-6), 155–160 (2002).
12. Y. Barad, H. Eisenberg, M. Horowitz, and Y. Silberberg, "Nonlinear scanning laser microscopy by third harmonic generation," Appl. Phys. Lett. **70**(8), 922 (1997).
13. C. Conti, A. Butsch, F. Biancalana, and P. S. J. Russell, "Dynamics of optomechanical spatial solitons in dual-nanoweb structures," Phys. Rev. A **86**(1), 013830 (2012).
14. J. S. Levy, M. A. Foster, A. L. Gaeta, and M. Lipson, "Harmonic generation in silicon nitride ring resonators," Opt. Express **19**(12), 11415–11421 (2011).

#252937 Received 29 Oct 2015; revised 13 Jan 2016; accepted 16 Jan 2016; published 21 Jan 2016

15. T. Ning, O. Hyvärinen, H. Pietarinen, T. Kaplas, M. Kauranen, and G. Genty, "Third-harmonic UV generation in silicon nitride nanostructures," Opt. Express **21**(2), 2012–2017 (2013).
16. R. Halir, Y. Okawachi, J. S. Levy, M. A. Foster, M. Lipson, and A. L. Gaeta, "Ultrabroadband supercontinuum generation in a CMOS-compatible platform," Opt. Lett. **37**(10), 1685–1687 (2012).
17. D. T. H. Tan, K. Ikeda, P. C. Sun, and Y. Fainman, "Group velocity dispersion and self phase modulation in silicon nitride waveguides," Appl. Phys. Lett. **96**(6), 061101 (2010).
18. C. Huang and L. Zhu, "Enhanced optical forces in 2D hybrid and plasmonic waveguides," Opt. Lett. **35**(10), 1563–1565 (2010).
19. J. Kischkat, S. Peters, B. Gruska, M. Semtsiv, M. Chashnikova, M. Klinkmüller, O. Fedosenko, S. Machulik, A. Aleksandrova, G. Monastyrskyi, Y. Flores, and W. Ted Masselink, "Mid-infrared optical properties of thin films of aluminum oxide, titanium dioxide, silicon dioxide, aluminum nitride, and silicon nitride," Appl. Opt. **51**(28), 6789–6798 (2012).
20. H. R. Philipp, "Optical properties of silicon nitride," ECS J. Solid State Sci. Technol. **120**, 295–300 (1973).
21. J. J. Vlassak and W. D. Nix, "A new bulge test technique for the determination of Young's modulus and Poisson's ratio of thin films," J. Mater. Res. **7**(12), 3242–3249 (1992).
22. M. L. Povinelli, M. Loncar, M. Ibanescu, E. J. Smythe, S. G. Johnson, F. Capasso, and J. D. Joannopoulos, "Evanescent-wave bonding between optical waveguides," Opt. Lett. **30**(22), 3042–3044 (2005).
23. V. Grubsky and A. Savchenko, "Glass micro-fibers for efficient third harmonic generation," Opt. Express **13**(18), 6798–6806 (2005).
24. G. H. Shao, X. S. Song, F. Xu, and Y. Q. Lu, "Optical parametric amplification of arbitrarily polarized light in periodically poled LiNbO3," Opt. Express **20**(17), 19343–19348 (2012).
25. Z. Y. Yu, F. Xu, X. W. Lin, X. S. Song, X. S. Qian, Q. Wang, and Y. Q. Lu, "Tunable broadband isolator based on electro-optically induced linear gratings in a nonlinear photonic crystal," Opt. Lett. **35**(20), 3327–3329 (2010).
26. Z. Y. Yu, F. Xu, F. Leng, X. S. Qian, X. F. Chen, and Y. Q. Lu, "Acousto-optic tunable second harmonic generation in periodically poled LiNbO3," Opt. Express **17**(14), 11965–11971 (2009).
27. A. Butsch, F. Biancalana, C. Conti, and P. S. J. Russell, "Optomechanical self-channelling of light in freely suspended dual-planar-waveguide structure," in *2011 Conference on Lasers and Electro-Optics (CLEO)* (IEEE, 2011), paper QWE4.

## 1. Introduction

Optomechanics investigate the interaction of light field and mechanical motion in an integrated system. Optical forces play an important role in an optomechanical system, which have been proposed and demonstrated based on diverse configurations, for example, a suspended Fabry-Perot cavity or high-finesse micro resonators with the radiation-pressure force [1] and an evanescently coupled sub-wavelength waveguide device with the transverse gradient force [2]. In the evanescently coupled configuration, the force originated from the lateral gradient of a propagating light, can be used directly to lead to the deformation of optical waveguides and devices [3, 4]. Compared with the radiation pressure force, the transverse force can save the reflective mirrors and it is more attractive and versatile for operation in planar structures.

Optomechanical devices based on the transverse gradient force, generally consist of a substrate and a suspended waveguide [5] or two parallel waveguides [6]. The deformation contributes to the effective index change and has been widely used to tune the linear characteristics such as phase, coupling and birefringence. Related devices have been widely studied including tunable directional couplers [7], all-optical switching devices [8], tunable birefringence devices [6]. Moreover, the optical force induced effective-index-change will also have a great influence on the nonlinear frequency conversion based on various phase-matching techniques which offers an effective way to expand the laser wavelength range, including second harmonic generation (SHG), third harmonic generation (THG), high harmonic generation, four-wave mixing (FWM), sum frequency generation and difference frequency generation.

In silicon/silica based optoelectronics devices, only third-order optical nonlinearities are present owing to its crystalline inversion symmetry, but in fact SHG can be realized based on the surface effect or external electrical field. So far, SHG and THG have been demonstrated in numerous fiber and planar waveguide devices [9, 10]. However, little attention has been paid to them in the optomechanical devices based on the transverse gradient force. In this paper, we investigate the impact of optical gradient forces on nonlinear frequency conversion by

#252937 Received 29 Oct 2015; revised 13 Jan 2016; accepted 16 Jan 2016; published 21 Jan 2016

harmonic generation in two coupled nanoscale waveguides. Induced by the electromagnetic field around waveguides, the optical forces lead to deformation between the coupled waveguides. Then the effective refractive index and phase-matching condition change as well. The phase-matching wavelength shifts with the input light power. Our simulation shows that the third harmonic phase-matching wavelength shifts 90 nm (3.6 nm/mW) along the waveguides, when the power increases to 25 mW with a waveguide length of 100 μm and an initial gap of 150 nm respectively. Moreover, for the case of a single-frequency pump, the conversion efficiency oscillates with the pump wavelength and power, and the optimal phase-matching wavelength red-shifts ~50 nm. This has plenty of important applications, such as all optical full logic unit [11], all-optical control, nonlinear scanning laser microscopy [12] and broadband nonlinear frequency conversion .

## 2. Optical forces and deformation

The waveguide structure we studied in this paper is shown in Fig. 1, which is two parallel, suspended waveguides separated by a distance $d$ with a free-standing section of length $L$. Each waveguide has a cross section of dimensions $w \times h$. In real devices, both ends of the waveguides have to rest on a substrate which is the most common configuration in planar waveguides. Otherwise, both sides of the waveguides can be attached to a wall [13], which is only shown inside a capillary fiber with a suspended dual-nanoweb structure. Here we consider the case of two silicon nitride waveguides with fixing two ends, and assume the width and height of the waveguide are 700 nm and 400 nm. The refractive index of silicon nitride is between silica and silicon. Because of the tunability of its refractive index, silicon nitride comes to become an important CMOS material. So far, it has been demonstrated THG [14, 15], supercontinuum generation [16] and self-phase modulation [17] in silicon nitride structures.

The force on the free-standing waveguides arises when the guided light is coupled to each other, and the magnitude of the force depends on the wavelength, power of light propagating in the waveguides, and the waveguide separation. The force can be calculated as a function of wavelength using the Maxwell Stress Tensor formulation, shown as an integral expression over the electric and magnetic fields of the two waveguides [18]:

$$\begin{aligned}\langle F\rangle &= \left\langle \iint \left(\bar{T}\cdot\hat{n}\right) dA \right\rangle \\ &= \int_L \left\{ \frac{\varepsilon}{2}\mathrm{Re}\left[\left(E\cdot\hat{n}\right)E^*\right] - \frac{\varepsilon}{4}\left(E\cdot E^*\right)\hat{n} + \frac{\mu}{2}\mathrm{Re}\left[\left(H\cdot\hat{n}\right)H^*\right] - \frac{\mu}{4}\left(H\cdot H^*\right)\hat{n} \right\} dl,\end{aligned} \tag{1}$$

where $\varepsilon$ and $\mu$ are the dielectric constant and permittivity, respectively, $\hat{n}$ is the outward unit normal to the surface, $E$ and $H$ are the electric and magnetic field distributions. In this paper, the electric and magnetic field distributions are calculated based on the finite-element method (FEM), taking the material dispersion of silicon nitride into account [19, 20].

#252937 Received 29 Oct 2015; revised 13 Jan 2016; accepted 16 Jan 2016; published 21 Jan 2016

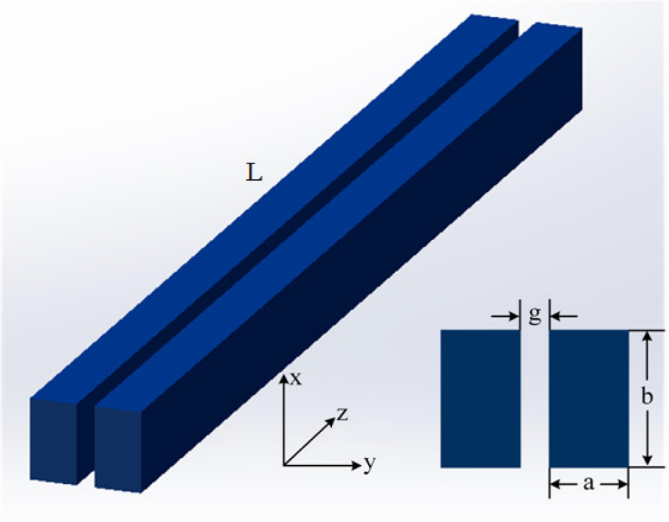


Fig. 1. Schematic of two parallel, suspended silicon nitride waveguides with fixed edges and its cross section, where $a$ = 400 nm, $b$ = 700 nm, $g$ = 150 nm, $L$ = 100 μm.

The optical force pulls the waveguides towards each other and the deformation along the waveguide because of the force is decided by the following deformation equation [5]

$$EI\frac{d^4u(z)}{dz^4} = -q(z), \tag{2}$$

where $E$ = 222 GPa is the young's modulus of silicon nitride [21], $I = \frac{ba^3}{12}$ is the waveguide's moment of inertia, $u$(z), $z$ and $q(z)$ are the deformation distribution, the direction and the optical force per unit length along the waveguide, respectively.

From the deformation equation above, we can get deformation of different positions. When the waveguide deforms, the gap between the two waveguides changes, and then optical forces transform as well with different gap. This in turn influences the deformation. Finally, the displacement of each waveguide is a function of position along the waveguide [22]. In order to obtain a convergent solution of ordinary differential Eq. (2), an iterative algorithm is introduced. The iterative loop terminates when the waveguide deformation converges to one millionth.

### 3. Phase-matching wavelength tuning

Efficient THG requires the satisfaction of the phase-matching condition, where is the propagating constant $\Delta\beta = 0$. In optical waveguides, the phase-matching condition can be reached if the modal dispersion compensates the material dispersion. For the parallel, suspended waveguides with fixed edges, the intermodal phase-matching involving is possibly satisfied with the same effective index between the fundamental mode of the fundamental wave (FW) and the higher-order mode of the third harmonic (TH) at an appreciate wavelength. This condition is only satisfied for certain wavelength or waveguide size and provides extremely small bandwidths.

When the pump power is weak enough, and we do not take the deformation of the waveguides into account, the gap is constant (gap = 150 nm) along the waveguides. Therefore the phase-matching condition is changeless and we can get initial phase-matching wavelength of $\lambda_i$ = 1632 nm in the whole waveguides. However, the optical force deforms the waveguides when the power increases and the effective refractive index of both the FW($n_{eff}(\omega)$) and

#252937 Received 29 Oct 2015; revised 13 Jan 2016; accepted 16 Jan 2016; published 21 Jan 2016

TH($n_{eff}(3\omega)$) changes. Those lead to the change of the phase-matching condition and the shift of the phase-matching wavelength along the waveguides. The deformation distribution can be calculated by solving Eq. (2) and the maximum of the deformation always occurs at the center of the waveguides. Figure 2 shows the calculated phase-matching wavelength shift and the gap at the position of the maximum waveguide deformation.

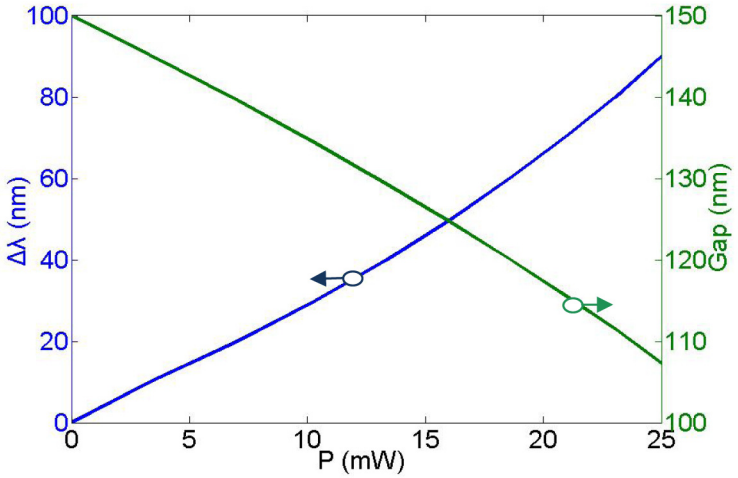


Fig. 2. Tuning the phase-matching wavelength shift at the position with maximum deformation by adjusting input power. The figure also shows the relationship between gap and input power. Δλ is the tuning range of phase-matching wavelength.

As shown in Fig. 2, when the change of input power is 25 mW, the phase-matching wavelength at the position with the maximum deformation shifts as large as 90 nm. It means that the optically-actuated device can permit phase matching over a tunable and wide bandwidth along the waveguides, which is useful for wideband pumps. Moreover, the longer the initial waveguide length is, the larger the deformation changes at the same input power, and the bigger the phase-matching wavelength shifts, which can be seen in Fig. 3.

For the case of the dual-web fiber, the waveguide can deform with the input power, and the phase-matching wavelength shifts, too. However, it is different because the deformation and the phase-matching wavelength are uniform along the fiber and it is beneficial to match a narrow-bandwidth pump source and obtain effective THG by tuning the input power.

#252937 Received 29 Oct 2015; revised 13 Jan 2016; accepted 16 Jan 2016; published 21 Jan 2016

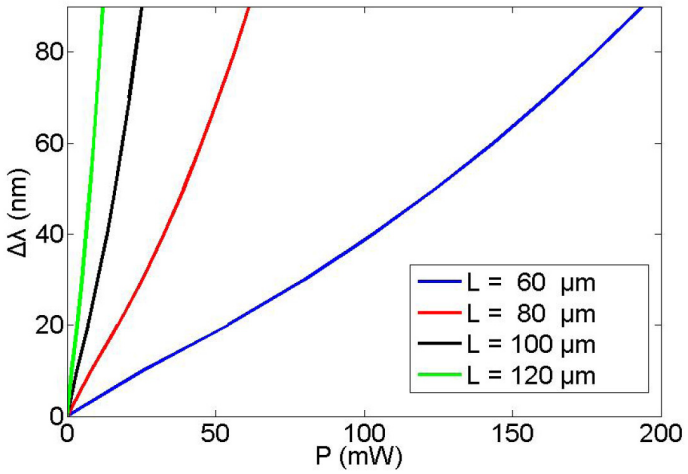


Fig. 3. The relationship between Δλ and input power P for coupled waveguides with different length parameters.

In practical applications, the environment temperature and the input power change all the time and they result in the optical force fluctuations. It is inevitable, but can be depressed by utilizing highly stable pump source and highly precise temperature controller. We also calculate their influences. For example, when the input power changes 1%, which changes from 10 mW to 10.1mW, the phase-matching wavelength shifts ~0.3 nm. When the environment temperature changes 1°C, the phase-matching wavelength shifts ~0.1nm.

## 4. Conversion efficiency

When a single-frequency pump propagates through the waveguides, the optical force will deform the waveguides. As the differences of deformation degree along the waveguides, the phase mismatch between the pump and the harmonic is not uniform as shown in Fig. 4. The conversion efficiency depends on the whole mismatch along the waveguides.

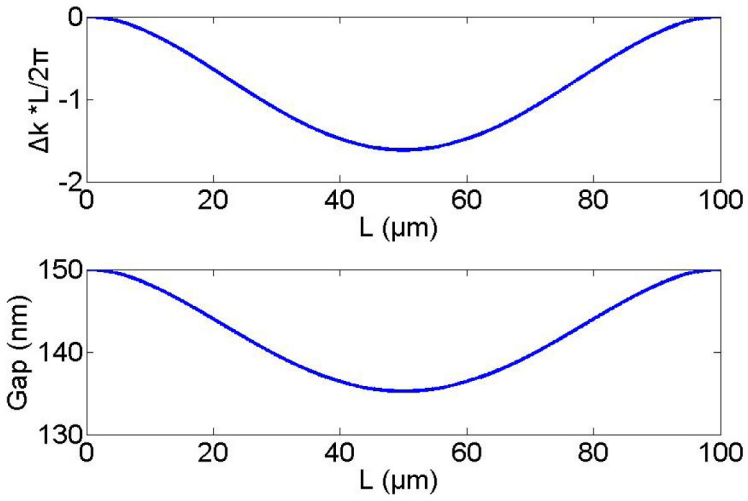


Fig. 4. The phase mismatch and gap along the waveguides with a single-frequency pump (1632 nm) at 10 mW.

The conversion efficiency of THG is expressed as [23],

#252937 Received 29 Oct 2015; revised 13 Jan 2016; accepted 16 Jan 2016; published 21 Jan 2016

$$\eta = \frac{P_{out}}{P_{in}} \propto \eta_p = \left( \int_0^L e^{-i \cdot \Delta\beta \cdot z} dz \right)^2 \cdot P_{in}^2. \quad (3)$$

We define the normalized conversion efficiency $\eta_n = \eta_p / P_{in}^2$ and $\eta_n = 1$ is the maximum when the phase-matching condition is always satisfied along the waveguides. For the optomechanical waveguides, it is not possible to achieve $\eta_n = 1$ because of the nonuniform deformation.

Figure 5(a) shows $\eta_p$ is oscillating with the pump power. When the pump power is close to zero, the deformation is ignorable and the maximum $\eta_p$ is achieved at the initial phase-matching wavelength $\lambda_i$. When the power increases, the equivalent phase-matching wavelength with the maximum $\eta_p$ red-shifts because of the serious deformation. Figure 5(b) shows that the maximum $\eta_p$ is oscillating upward and then downward with the pump wavelength. The optimal phase-matching wavelength at the turning point is $\delta\lambda$ ~50 nm.

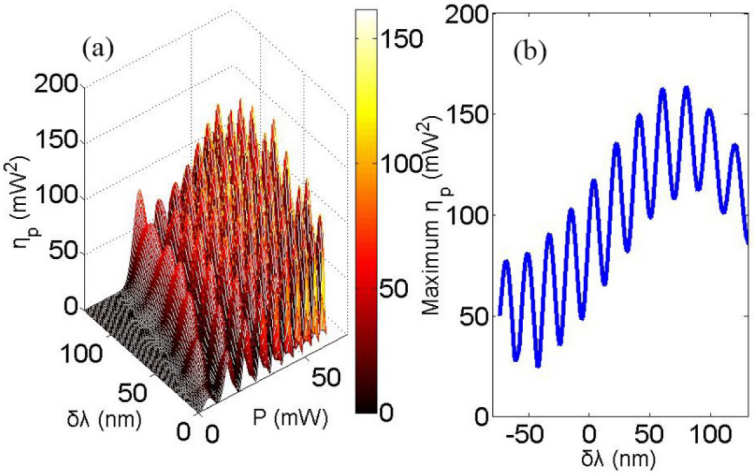


Fig. 5. (a) 3D graph of $\eta_p$ with different input wavelength and input power. δλ is the difference between the input wavelength and the initial phase-matching wavelength $\lambda_i$. (b) The relationship between the maximum $\eta_p$ and δλ. We choose the maximum value of $\eta_p$ at certain input wavelength as the maximum $\eta_p$ with the input power ranging from 0 mW to 60 mW.

## 5. Discussion

Conventional approaches to tuning the phase-matching wavelength utilize electro-optic [24, 25], thermal-optic and acousto-optic effects [26]. Additional experimental instruments, for example, a voltage supplier, have to be employed. In our paper, we mainly concentrate on the influence of optical forces on nonlinear optical frequency conversion. At the same time, it provides an alternative method for all-optical control of nonlinear optical frequency conversion. In addition, we can attain a wide range of phase-matching wavelength tuning. However, it needs suspend waveguides which are more difficult to be fabricated and the conversion efficiency seriously oscillates with the pump power.

## 6. Conclusion

In this paper, we theoretically investigate the impact of optical gradient forces on nonlinear frequency conversion, especially concentrating on the phase-matching wavelength and conversion efficiency, in two coupled waveguides. The gap between two waveguides can be changed by adjusting the input power, and then the phase-matching condition is changed and the phase-matching wavelength shifts along the waveguides. When the input power is 25 mW, the phase-matching wavelength shifts 90 nm (3.6 nm/mW). It means that the optically-

#252937 Received 29 Oct 2015; revised 13 Jan 2016; accepted 16 Jan 2016; published 21 Jan 2016

actuated device can permit phase matching over a tunable and wide bandwidth along the waveguides, which is useful for wideband pumps.

What is more, the optical forces also have impact on conversion efficiency for a single-frequency pump. The pump-induced deformation is not uniform along the waveguide and it results in the drop of the normalized conversion efficient. The equivalent phase-matching wavelength red-shifts when the pump power increases. The maximum conversion efficiency can be achieved at an optimal phase-matching wavelength with a shift of 50 nm.

We all believe that we can enhance the conversion efficiency and attain wider range of phase-matching wavelength tuning by changing waveguide structure, just like dual-web fiber [13, 27], to make the deformation uniformly along the waveguide, which it is always phase-matching.

**Acknowledgments**

This work is sponsored by National 973 program (2012CB921803), and National Natural Science Foundation of China (61322503, 61225026, and 61475069).

#252937 Received 29 Oct 2015; revised 13 Jan 2016; accepted 16 Jan 2016; published 21 Jan 2016